Catalysis Letters
https://doi.org/10.1007/s10562-019-03083-0

Immobilized *N*-Heterocyclic Carbene-Palladium(II) Complex on Graphene Oxide as Efficient and Recyclable Catalyst for Suzuki–Miyaura Cross-Coupling and Reduction of Nitroarenes

Vishal Kandathil[1] · Bhakti Kulkarni[1] · Aisha Siddiqa[1] · Manjunatha Kempasiddaiah[1] · B. S. Sasidhar[2] · Shivaputra A. Patil[3] · Siddappa A. Patil[1]

Received: 26 October 2019 / Accepted: 15 December 2019

Abstract

A new and efficient *N*-heterocyclic carbene (NHC)-palladium(II) complex immobilized on graphene oxide (NHC-Pd@GO) has been successfully designed and synthesized. The prepared NHC-Pd@GO heterogeneous catalyst was fully characterized using a combination of fourier transform infrared spectroscopy (FTIR), inductively coupled plasma-optical emission spectroscopy (ICP-OES), energy-dispersive X-ray spectroscopy (EDS), field-emission scanning electron microscopy (FESEM), transmission electron microscopy (TEM), X-ray powder diffraction (XRD), thermogravimetric analysis (TGA) and Brunauer–Emmett–Teller surface area analysis (BET). This new air- and moisture-stable NHC-Pd@GO heterogeneous catalytic system was found to be a highly active catalyst in the Suzuki–Miyaura cross-coupling between phenylboronic acid and various aryl halides (bromides/chlorides/iodides) and in the reduction of nitroarenes. These organic transformations were best performed in an aqueous ethanol and aqueous methanol solvent system respectively with low catalyst loading under mild reaction conditions. Furthermore, NHC-Pd@GO heterogeneous catalyst could be recovered easily and reused at least eleven times in Suzuki–Miyaura cross-coupling and nine times in reduction of nitroarenes without any considerable loss of its catalytic activity. The stability and good selectivity of the NHC-Pd@GO heterogeneous catalyst in recycling experiments signify that it could be useful for practical application in various organic transformations.

Vishal Kandathil and Bhakti Kulkarni have contributed equally.

✉ Siddappa A. Patil
p.siddappa@jainuniversity.ac.in; patilsiddappa@gmail.com

[1] Centre for Nano and Material Sciences, Jain University, Jain Global Campus, Kanakapura, Ramanagaram, Bangalore, Karnataka 562112, India

[2] Organic Chemistry Section, Chemical Sciences & Technology Division, National Institute for Interdisciplinary Science and Technology (CSIR), Thiruvananthapuram, Kerala 695019, India

[3] Pharmaceutical Sciences Department, College of Pharmacy, Rosalind Franklin University of Medicine and Science, 3333 Green Bay Road, North Chicago, IL 60064, USA

Graphic Abstract

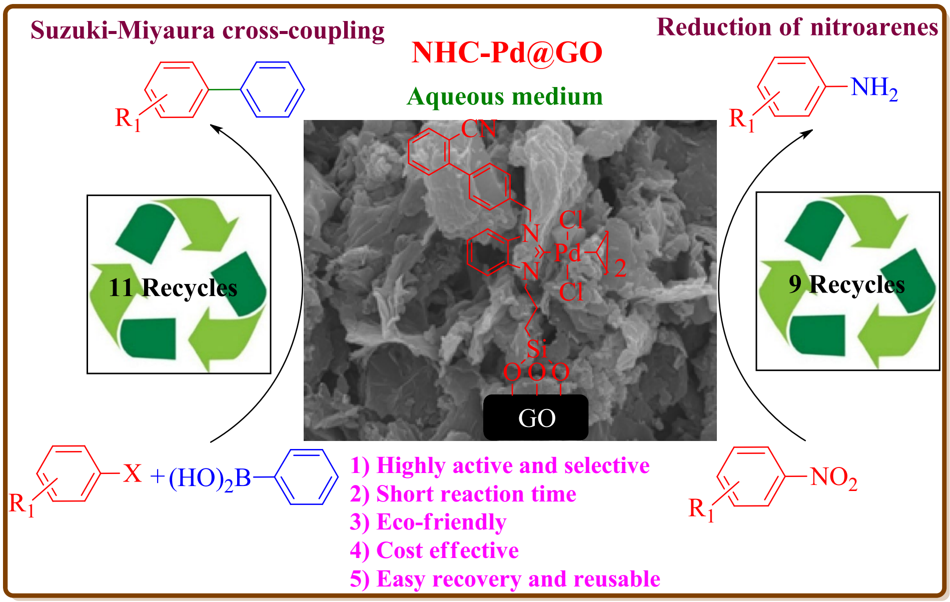

Keywords Graphene oxide · *N*-heterocyclic carbene-palladium(II) · Heterogeneous catalysis · Suzuki–Miyaura cross-coupling · Nitroarene reduction

1 Introduction

In recent years, Suzuki–Miyaura cross-coupling reaction plays an important role towards the generation of new carbon–carbon (C–C) bonds in both academic and industrial sectors. Suzuki–Miyaura cross-coupling reaction involves the transition metal palladium catalyzed cross-coupling of organoboronic acids with organic halides [1–4]. Suzuki–Miyaura cross-coupling reaction has been applied to the synthesis of numerous organic compounds like pharmaceutical drugs, liquid crystals, molecular wires, conducting polymers, complex natural products and in supramolecular chemistry [4–11]. Consequently, huge efforts have been done to the development of homogeneous ligand systems for Suzuki–Miyaura cross-coupling reaction such as diazabutadienes, *N*-heterocyclic carbenes (NHCs), amines, imines, oxime palladacycles and phosphines [12–17]. Conversely, synthesis of aromatic amines through the reduction of nitroarenes is an important concern in the preparation of dye intermediates, agrochemicals, photographic chemicals, polymers, rubber chemicals, pigments and pharmaceuticals [18]. The common methods to synthesize the amines are based on; (i) amination of various functional groups (OH, H, F, Cl, Br, I etc.) through the corresponding diazonium salts and (ii) reduction of nitro compounds with homogeneous catalysts [19–22]. Hence, the uses of transition metal complexes in the form of homogeneous catalysts have tremendously increased for numerous organic transformations. Nevertheless, most important drawback of homogeneous catalysts is the difficulty in their recovery and reuse from the reaction medium. This problem is of economic and environmental concern in bulk-scale syntheses.

In recent years, NHC-metal complexes have been successfully used as catalyst for numerous organic transformations [23, 24]. Stable NHC-metal complexes have been effortlessly prepared from various transition metal ions with different oxidation states. Of late, various types of NHC-palladium(II) complexes have been developed as heterogeneous catalysts for various organic transformations through immobilizing palladium(II) on various solid supports [25–29]. Regrettably, these heterogeneous catalysts habitually suffer from many difficulties such as inferior selectivity, reduced activity and many more problems such as preparation complexity and metal leaching.

In this regard, graphene oxide (GO) has attracted wide interest in heterogeneous catalysis because of its distinctive properties such as huge surface area, two-dimensional structure, easy recovery and recycling [30, 31]. In addition, graphene oxide is largely oxygenated with hydroxyl, epoxide, carbonyl and carboxyl groups which provide plenty of opportunities for functionality modifications as active sites for tethering metal ions and complexes for efficient chemical transformation. Hence, GO has been recognized as best candidate for attaching many transition metal complexes

[32–34]. Fan et al. prepared a novel GO tethered palladium complex catalyst through immobilizing palladium(II) on the surface of GO for the Suzuki–Miyaura cross-coupling reaction of aryl halides and phenylboronic acid. The catalyst exhibited high activity and could be recycled and reused numerous times without significant loss of activity [35]. Khatri et al. prepared rhenium-oxo Schiff-base complex on GO nanosheets for the oxidation of numerous amines under mild reaction conditions [36]. Mungse et al. reported oxo-vanadium Schiff-base complex attached on the surface of GO as a heterogeneous catalyst for the oxidation of alcohols which exhibited high catalytic activity [37].

Generally, NHCs are stabilized through bulky substituents on the nitrogen atoms. Hence, we have chosen 4′-bromomethyl-2-biphenylcarbonitrile for substitution on one nitrogen and (3-chloropropyl)triethoxysilane attached GO on the other nitrogen. In addition, the strong affinity of GO towards silica makes silanes very useful for the functionalization of GO. In a continuation of our very recent investigations of the applications of heterogeneous catalysts in C–C cross-coupling and reduction of nitroarenes reactions [38–42], herein we report the synthesis and characterization of *N*-heterocyclic carbene-palladium(II) complex immobilized on GO (NHC-Pd@GO). This new air- and moisture-stable heterogeneous catalyst was found to be highly active in Suzuki–Miyaura cross-coupling and reduction of nitroarenes reactions in an aqueous ethanol and aqueous methanol as green solvents using an extremely small amount of palladium under mild conditions (room temperature and short reaction time). Furthermore, NHC-Pd@GO heterogeneous catalyst could be easily recovered from the reaction media by simple filtration and reused at least 12 and ten cycles in the Suzuki–Miyaura cross-coupling and reduction of nitroarenes respectively without significant loss of its activity.

2 Experimental

2.1 Materials

All solvents were purified according to standard methods prior to use. Unless otherwise stated, all reactions were performed under aerobic conditions in oven-dried glassware with magnetic stirring. Graphite, $NaNO_3$, H_2SO_4, H_2O_2, $KMnO_4$, benzimidazole, 4′-bromomethyl-2-biphenylcarbonitrile, palladium(II) acetate, (3-chloropropyl)triethoxysilane, aryl halides, bases, and phenylboronic acid were purchased from Avra and Sigma-Aldrich chemical company and were used without further purification. Heating was accomplished by either a heating mantle or silicone oil bath. Column chromatography was conducted on silica gel 60–120 mesh (Merck) and thin layer chromatography was carried out using 0.25 mm Merck TLC silica gel plates with UV light as a visualizing agent. Yields refer to chromatography pure material. Concentration in vacuo refers to the removal of volatile solvent using a rotary evaporator attached to a dry diaphragm (10–15 mm Hg) followed by pumping to a constant weight with an oil pump (< 300 mTorr). All the organic products were known and identified by comparison of their spectral data with those of authentic samples.

2.2 Characterization

Fourier transform infrared spectra (FTIR) were recorded with a PerkinElmer Spectrum Two spectrometer. Brunauer–Emmett–Teller (BET) surface areas were obtained by physisorption of nitrogen using a Microtrac BELSORP-MAX instrument. The elemental palladium content of the nanomagnetic catalyst was determined with a Perkin Elmer Optima 5300 DV inductively coupled plasma optical emission spectrometer (ICP-OES). Transmission electron microscopy (TEM) images were obtained using a Jeol/JEM 2100 microscope. Field-emission scanning electron microscopy (FESEM) along with energy-dispersive X-ray spectroscopy (EDS) to observe morphology and determine elemental distributions, respectively, were conducted with a JEOL model JSM7100F. Thermogravimetric analysis (TGA) was carried out with a PerkinElmer Diamond TG/DTA with a heating rate of 10.0 °C min^{-1}. Powder X-ray diffraction (XRD) patterns were obtained using a Bruker AXS D8 Advance. ^1H NMR spectra were recorded at 400 MHz, and are reported relative to deuterated chloroform ($CDCl_3$; $\delta = 7.27$ ppm). ^1H NMR coupling constants (J) are reported in hertz (Hz) and multiplicities are indicated as follows: s (singlet), d (doublet), t (triplet), m (multiplet).

2.3 Synthesis of Graphene Oxide (GO) (1)

Graphene oxide was synthesized and purified according to modified Hummers method from readily available graphite. In a typical experiment, conc. H_2SO_4 (23 mL) was added to the mixture of graphite (1.0 g) and $NaNO_3$ (0.5 g) in a round bottomed flask (250 mL) and the resulting reaction mixture was cooled down to 0 °C in an ice bath under stirring for 2 h. Then $KMnO_4$ (3.0 g) was slowly added to the above reaction mixture with vigorous stirring and the flask was kept for oxidizing at 0 °C for another 2 h. Afterward, the reaction mixture was transferred to a pre-heated water bath at 35 °C and stirring was continued for further 2 h. Water (H_2O) (50 mL) was slowly added into the reaction system and the temperature was increased to 95 °C for 15 min. Then reaction mixture was treated with 30% H_2O_2 (10 mL) and resulting solid was filtered, washed with 5% HCl and deionized water until the pH reached neutral. The obtained solid was dried at 70 °C till constant weight to get pure GO.

2.4 Synthesis of Silyl Chloride Functionalized Graphene Oxide (3)

The synthesised graphene oxide (2.0 g) was suspended in ethanol (EtOH) (125 mL) through ultrasonicating for 30 min. Ammonia was added to the suspension and stirred at 40 °C for 3 h. Then (3-chloropropyl)triethoxysilane (8 mL) was added to the above reaction solution and stirring was continued for further 8 h at 40 °C. Then, reaction solution was cooled to room temperature. The obtained black precipitate was collected by centrifugation and washed with EtOH (3 × 25 mL) followed by H_2O (1 × 25 mL) and dried at 40 °C for 12 h.

2.5 Synthesis of 4′-((1*H*-benzo[d]imidazol-1-yl)methyl)-[1,1′-biphenyl]-2-carbonitrile (6)

A mixture of benzimidazole (0.5 g, 4.23 mmol) and potassium hydroxide (0.34 g, 6.06 mmol) in DMSO (20 mL) was stirred at 100 °C for 2 h. The temperature of the reaction mixture was reduced to room temperature and 4′-bromomethyl-2-biphenylcarbonitrile (1.15 g, 4.23 mmol) was added and stirring was continued for further 12 h. Then reaction mixture was poured into ice-cold water. The precipitated solid product was washed with water and dried at 40 °C in vacuo for 4–5 h to yield 4′-((1*H*-benzo[d]imidazol-1-yl)methyl)-[1,1′-biphenyl]-2-carbonitrile as an off-white solid. Yield: 92%. 1H NMR (400 MHz, $CDCl_3$) δ 8.03 (s, 1H), 7.88 (d, *J* = 6.7 Hz, 1H), 7.78 (s, 1H), 7.66 (s, 1H), 7.56 (d, *J* = 8.1 Hz, 2H), 7.49 (d, *J* = 7.8 Hz, 2H), 7.38 – 7.28 (m, 5H), 5.47 (s, 2H).

2.6 Synthesis of Graphene Oxide Tethered *N*-Heterocyclic Carbene (NHC@GO) (7)

A mixture of 4′-((1*H*-benzo[d]imidazol-1-yl)methyl)-[1,1′-biphenyl]-2-carbonitrile (2 g, 6.47 mmol) and silyl chloride functionalized graphene oxide (4 g) in toluene (60 mL) was sonicated for 30 min. The reaction mixture was kept for stirring at 110 °C for about 48 h. Then, reaction mixture was cooled to room temperature. The obtained black precipitate was collected by centrifugation, washed with fresh toluene (3 × 40 mL) and dried at 40 °C in vacuo for 12 h to yield graphene oxide tethered *N*-heterocyclic carbene.

2.7 Synthesis of Graphene Oxide Tethered *N*-Heterocyclic Carbene-Palladium(II) Complex (NHC-Pd@GO) (8)

To a solution of Na_2CO_3(0.5 M, 30 mL) in dimethylformamide (DMF) (30 mL), palladium(II) acetate (0.33 g, 1.47 mmol) was added and the reaction mixture was stirred at room temperature for 10 min. Then graphene oxide attached *N*-heterocyclic carbene was added to the above reaction mixture and stirring was continued at 50 °C for 16 h. The reaction mixture was then cooled to room temperature. The resultant product was isolated by centrifugation, washed with distilled water (2 × 40 mL) and dried at 40 °C in vacuo for 12 h to yield graphene oxide tethered *N*-heterocyclic carbene-palladium(II) complex (NHC-Pd@GO).

2.8 General Procedure for Suzuki–Miyaura Cross-Coupling Reaction

A mixture of aryl halide (0.27 mmol), phenylboronic acid (1 mmol), NHC-Pd@GO heterogeneous catalyst (0.01 g) and potassium carbonate (1.1 mmol) was stirred in EtOH:H_2O (1:1) solvent system at room temperature for designated hours. The progress of the reaction was monitored by TLC. After reaction completion, the mixture was cooled to room temperature and NHC-Pd@GO heterogeneous catalyst was separated through centrifugation. To the filtrate, dichloromethane and water were added. Dichloromethane layer was separated from the water layer using a separatory funnel and dried with magnesium sulphate. The dried dichloromethane was concentrated in vacuum and obtained crude product was purified from column chromatography over silica gel using hexane and ethyl acetate as eluting solvent to get the corresponding products in good to excellent yields. All the coupled products were known molecules and were confirmed by comparing the ^1H NMR spectral data with those of authentic samples.

1. *[1,1′-Biphenyl]-4-carbonitrile* (Table 7, entry 1): ^1H NMR (400 MHz, $CDCl_3$) δ 7.74–7.71 (m, 2H), 7.70–7.67 (m, 2H), 7.59 (d, *J* = 5.3 Hz, 2H), 7.48 (d, *J* = 8.1, 6.7 Hz, 2H), 7.43 (d, *J* = 7.3 Hz, 1H).
2. *1,1′-Biphenyl* (Table 7, entries 2 and 11): ^1H NMR (400 MHz, $CDCl_3$) δ 7.60 (d, *J* = 7.7 Hz, 4H), 7.44 (t, *J* = 7.5 Hz, 4H), 7.35 (t, *J* = 7.2 Hz, 2H).
3. *[1,1′-Biphenyl]-4-ol* (Table 7, entries 3, 15 and 16): ^1H NMR (400 MHz, $CDCl_3$) δ 7.54 (d, *J* = 8.3 Hz, 2H), 7.50– 7.44 (m, 2H), 7.41 (d, *J* = 10.6 Hz, 2H), 7.31 (d, *J* = 7.4 Hz, 1H), 6.94– 6.88 (m, 2H), 5.02 (s, 1H).
4. *1-([1,1′-Biphenyl]-4-yl)ethanone* (Table 7, entries 4 and 9): ^1H NMR (400 MHz, $CDCl_3$) δ 8.04 (d, *J* = 8.2 Hz, 2H), 7.69 (d, *J* = 8.2 Hz, 2H), 7.62 (s, 2H), 7.47 (d, *J* = 7.7 Hz, 2H), 7.41 (d, *J* = 7.1 Hz, 1H), 2.64 (s, 3H).
5. *[1,1′-Biphenyl]-4-carbaldehyde* (Table 7, entry 5): ^1H NMR (400 MHz, $CDCl_3$) δ 10.06 (s, 1H), 7.99–7.94 (m, 2H), 7.79–7.74 (m, 2H), 7.65 (d, *J* = 5.2 Hz, 2H), 7.52–7.45 (m, 2H), 7.43 (d, *J* = 4.9 Hz, 1H).
6. *4-Nitro-1,1′-biphenyl* (Table 7, entry 6): ^1H NMR (400 MHz, $CDCl_3$) δ 8.27 – 8.17 (m, 2H), 7.71–7.62

(m, 2H), 7.55 (d, $J = 5.3$ Hz, 2H), 7.46–7.39 (m, 2H), 7.39–7.34 (m, 1H).

7. *[1,1'-Biphenyl]-4-yl(phenyl)methanone* (Table 7, entry 7): ^{1}H NMR (400 MHz, $CDCl_3$) δ 7.92–7.88 (m, 2H), 7.86–7.82 (m, 2H), 7.71 (d, $J = 8.3$ Hz, 2H), 7.68–7.63 (m, 2H), 7.60 (t, $J = 7.4$ Hz, 1H), 7.49 (d, $J = 9.8$ Hz, 4H), 7.41 (t, $J = 7.4$ Hz, 1H).
8. *4-Methyl-1,1'-biphenyl* (Table 7, entries 8 and 12): ^{1}H NMR (400 MHz, $CDCl_3$) δ 7.57 (d, $J = 7.6$ Hz, 2H), 7.49 (d, $J = 7.3$ Hz, 2H), 7.41 (t, $J = 7.5$ Hz, 2H), 7.31 (t, $J = 7.3$ Hz, 1H), 7.24 (d, $J = 7.5$ Hz, 2H), 2.39 (s, 3H).
9. *4-Methoxy-1,1'-biphenyl* (Table 7, entries 10 and 13): ^{1}H NMR (400 MHz, $CDCl_3$) δ 7.58–7.51 (m, 4H), 7.41 (t, $J = 7.7$ Hz, 2H), 7.30 (t, $J = 7.4$ Hz, 1H), 6.98 (d, $J = 8.7$ Hz, 2H), 3.85 (s, 3H).
10. *[1,1'-Biphenyl]-2-carbaldehyde* (Table 7, entry 14): ^{1}H NMR (400 MHz, $CDCl_3$) δ 9.99 (s, 1H), 8.03 (d, $J = 7.8$ Hz, 1H), 7.65 (d, $J = 1.3$ Hz, 1H), 7.54–7.44 (m, 5H), 7.39 (d, $J = 7.7$ Hz, 2H).

2.9 General Procedure for Reduction of Nitroarenes

In a typical reduction reaction, nitroarene (0.81 mmol) was mixed with the NHC-Pd@GO heterogeneous catalyst (0.005 g) in MeOH:H_2O (1:1) (10 mL) solvent system and the reaction mixture was stirred for five minutes at room temperature. Consequently, $NaBH_4$ (1.62 mmol) was added to the reaction mixture and stirring was continued at room temperature for designated hours. The progress of the reaction was checked from TLC. After reaction completion, NHC-Pd@GO heterogeneous catalyst was separated through centrifugation and dichloromethane was added. The dichloromethane layer was separated from the water layer using a separating funnel and dried with anhydrous magnesium sulfate. The dried dichloromethane layer was concentrated in vacuum and obtained crude reduced product was purified through column chromatography over silica gel using hexane and ethyl acetate as eluting solvents to afford the pure products in good to excellent yields. All the reduced products were known molecules and were confirmed by comparing the ^{1}H NMR spectral data with those of authentic samples.

1. *Aniline* (Table 10, entry 1): ^{1}H NMR (400 MHz, $CDCl_3$) δ 7.14–7.07 (m, 2H), 6.72 (d, $J = 5.4$ Hz, 1H), 6.66–6.53 (m, 2H), 3.47 (s, 2H).
2. *Benzene-1,3-diamine* (Table 10, entry 2): ^{1}H NMR (400 MHz, $CDCl_3$) δ 7.66 (d, $J = 5.7$ Hz, 1H), 7.59–7.53 (m, 1H), 7.47 (d, $J = 5.7$ Hz, 1H), 7.38 (d, $J = 8.0$ Hz, 1H), 4.02 (s, 2H), 4.01 (s, 2H).
3. *4-Aminobenzaldehyde* (Table 10, entry 4): ^{1}H NMR (400 MHz, $CDCl_3$) δ 8.19 (s, 1H), 8.08 (d, $J = 8.2$ Hz, 1H), 7.64 (d, $J = 8.7$ Hz, 1H), 7.49–7.44 (m, 2H), 4.76 (s, 2H).
4. *2-Chloroaniline* (Table 10, entry 5): ^{1}H NMR (400 MHz, $CDCl_3$) δ 7.66 (d, $J = 5.7$ Hz, 1H), 7.47 (d, $J = 5.7$ Hz, 1H), 7.13 (d, $J = 7.6$ Hz, 1H), 7.00 (d, $J = 8.2$ Hz, 1H), 4.02 (s, 2H).
5. *4-Methoxyaniline* (Table 10, entry 6)**:** ^{1}H NMR (400 MHz, $CDCl_3$) δ 6.76–6.71 (m, 2H), 6.66–6.62 (m, 2H), 3.73 (s, 3H), 3.34 (s, 2H).
6. *m-Toluidine* (Table 10, entry 7): ^{1}H NMR (400 MHz, $CDCl_3$) δ 7.73 (d, $J = 5.7$ Hz, 1H), 7.54 (d, $J = 5.7$ Hz, 1H), 7.29 (d, $J = 2.4$ Hz, 1H), 7.07 (d, $J = 8.1$ Hz, 1H), 4.09 (d, $J = 6.7$ Hz, 2H), 2.27 (s, 3H).

2.10 Procedure for Recovery of Graphene Oxide Tethered *N*-Heterocyclic Carbene-Palladium(II) Complex (NHC-Pd@GO)

The stability and reusability of the catalyst are important concern in organic transformations particularly for convenient industrial applications. After the completion of reaction, NHC-Pd@GO heterogeneous catalyst was isolated from the reaction mixture by centrifugation. The separated NHC-Pd@GO heterogeneous catalyst was then washed with water (2 × 10 mL) followed by ethanol (2 × 10 mL) and dried at 45 °C for 12 h. Then dried NHC-Pd@GO heterogeneous catalyst was used for next round of Suzuki–Miyaura cross-coupling and reduction of nitroarenes without further purification.

3 Results and Discussion

3.1 Synthesis of Graphene Oxide Tethered *N*-Heterocyclic Carbene-Palladium(II) Complex

In continuation of our research work on the utilization of immobilized *N*-heterocyclic carbene-palladium(II) complex on different materials for various organic transformations [38, 39], herein, we report a facile and efficient method for Suzuki–Miyaura cross-coupling between a range of aryl halides with phenylboronic acid and also for the reduction of nitroarenes in the presence of catalytic amounts of NHC-Pd@GO heterogeneous catalyst.

The method for the synthesis of NHC-Pd@GO heterogeneous catalyst depicted in this work is outlined in Scheme 1. Initially, graphene oxide (**1**) was prepared and purified according to a modified Hummers method through easily accessible graphite. Then, silyl chloride functionalized graphene oxide (**3**) was synthesized by the functionalization of graphene oxide(**1**) with (3-chloropropyl) triethoxysilane (**2**) in EtOH at 40 °C in presence of ammonia. On the other hand, the intermediate 4′-((1*H*-benzo[d]

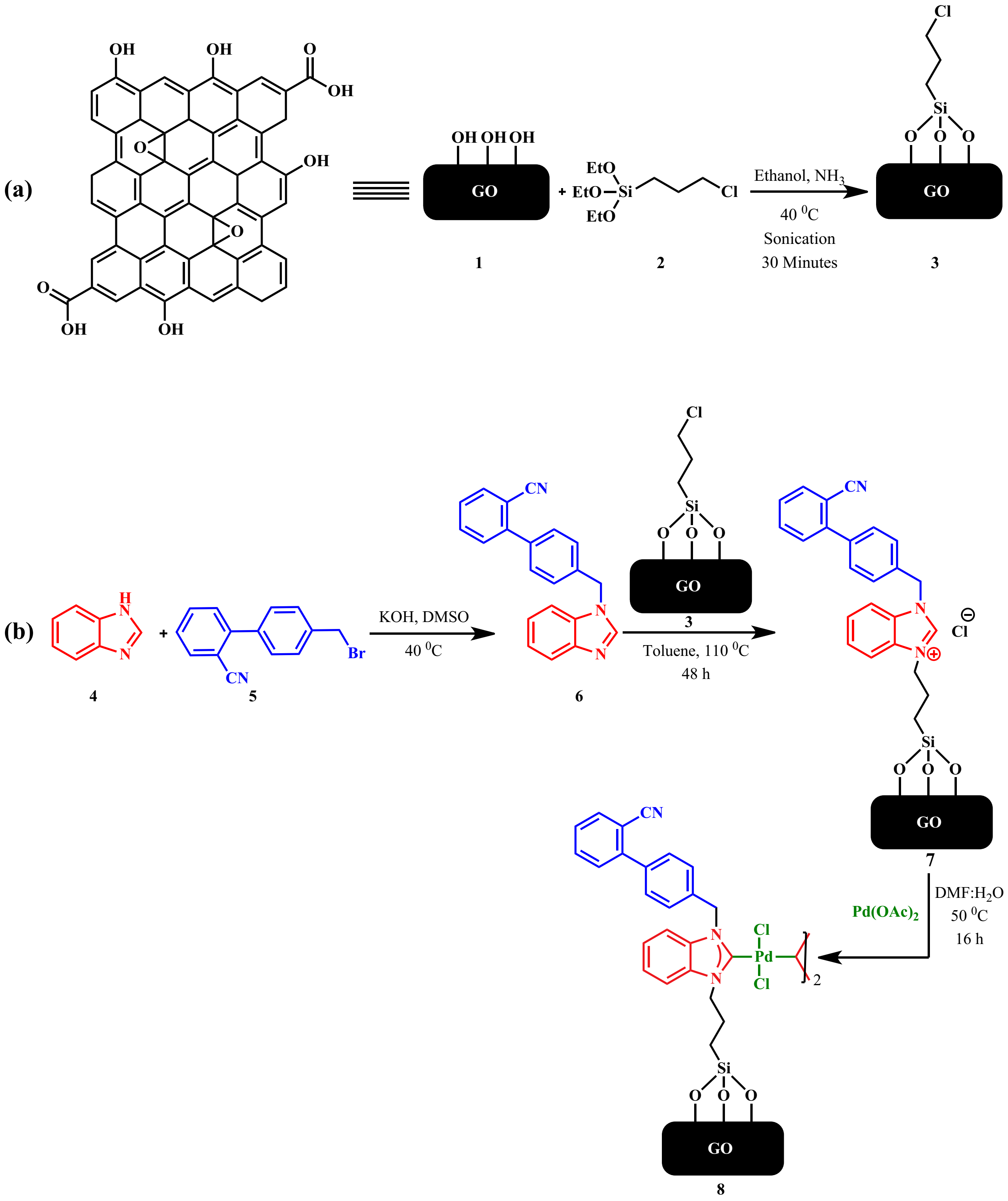

Scheme 1 Synthetic schemes for **a** silyl chloride functionalized graphene oxide (**3**) and **b** graphene oxide tethered *N*-heterocyclic carbene-palladium(II) complex (NHC-Pd@GO) (**8**)

imidazol-1-yl)methyl)-[1,1′-biphenyl]-2-carbonitrile (**6**) was prepared through the reaction of benzimidazole (**4**) with 4′-bromomethyl-2-biphenylcarbonitrile (**5**) in the presence of potassium hydroxide in DMSO. In the next step, 4′-((1*H*-benzo[d]imidazol-1-yl)methyl)-[1,1′-biphenyl]-2-carbonitrile (**6**) was treated with silyl chloride functionalized graphene oxide (**3**) in toluene at 110 °C for 48 h to get the corresponding graphene oxide tethered *N*-heterocyclic carbene (**7**). Finally, graphene oxide tethered *N*-heterocyclic carbene-palladium(II) complex (**8**) was synthesized through the coordination of palladium(II) acetate with graphene oxide tethered *N*-heterocyclic carbene (**7**).

3.2 Spectroscopic and Microscopic Characterization

The newly synthesized NHC-Pd@GO heterogeneous catalyst was characterized from attenuated total reflectance infrared spectroscopy, inductively coupled plasma-atomic emission spectroscopy, energy-dispersive X-ray spectroscopy, field-emission scanning electron microscopy, transmission electron microscopy, X-ray powder diffraction, thermogravimetric analysis and Brunauer–Emmett–Teller surface area analysis.

3.3 FTIR Spectroscopy

The structures of compounds from each step of the reaction were confirmed through fourier transform infrared spectroscopy. Figure 1a–e shows FTIR spectra of GO, 4′-((1*H*-benzo[d]imidazol-1-yl)methyl)-[1,1′-biphenyl]-2-carbonitrile, silane functionalized GO, graphene oxide tethered *N*-heterocyclic carbene and the NHC-Pd@GO heterogeneous catalyst. The FTIR spectrum of GO shows broad O–H bond stretching vibration at 3435.99 cm^{-1}, vibration of carboxyl group at 1627.64 cm^{-1} and C–O stretching vibration at 1094.57 cm^{-1}. The bands observed around 2221.63, 3024.82 and 1613.00 cm^{-1} (Fig. 1b) are ascribed to the carbonitrile, C–H and C=C stretching vibrations of the 4′-((1*H*-benzo[d]imidazol-1-yl)methyl)-[1,1′-biphenyl]-2-carbonitrile.The FTIR spectrum of silane functionalized GO reveals typical bands at 698.34, 2926.8 and 1128.09 cm^{-1} attributed to C–Cl stretching, aliphatic C–H stretching and Si–O–C stretching vibrations. The absence of C–Cl stretching peak around 700 cm^{-1} and the presence of carbonitrile, aliphatic and aromatic C–H stretching vibrations peaks at 2221.0, 3118.7 and 2852.7 cm^{-1} confirms the formation NHC@GO. The characteristic peaks at 2221.7, 2954.2 and 2921.11 cm^{-1} in the IR spectrum of the NHC-Pd@GO are due to carbonitrile, aliphatic and aromatic C–H stretching vibrations respectively, apart from the peak at 468.64 cm^{-1} which is due to C–Pd stretching which confirms the structure of the NHC-Pd@GO heterogeneous catalyst. Figure 2a–c shows the FTIR spectra of freshly prepared NHC-Pd@GO heterogeneous catalyst, 12 times recycled NHC-Pd@GO heterogeneous catalyst from Suzuki–Miyaura cross-coupling reaction and ten times recycled NHC-Pd@GO heterogeneous catalyst from the reduction of nitroarenes. Results demonstrate that the chemical composition of recycled NHC-Pd@GO heterogeneous catalyst from both the reactions is not visible apart from some slight shift in the peak positions.

3.4 Thermogravimetric Analysis

The thermal stability of GO and NHC-Pd@GO heterogeneous catalyst and organic functionalization on GO was inferred using TGA under nitrogen atmosphere from 35 to 800 °C at a rate of 10 °C per min. Figure 3a exhibited 15% weight loss in the range of 50–230 °C which is due to the loss of hydroxyl groups present on the surface of the GO and ~ 35% weight loss due to the pyrolysis of various oxygen containing functional groups. In contrast, the NHC-Pd@GO heterogeneous catalyst displayed higher thermal stability and the total weight loss of ~ 30% (Fig. 3b) shows the removal of organic moiety functionalized on the GO support. Furthermore, on the basis of TGA results, it is clear that NHC-Pd@GO heterogeneous catalyst is stable up to a temperature of 200 °C which in turn allows the usage of this NHC-Pd@GO heterogeneous catalyst in organic transformations carried out at higher temperatures.

3.5 BET Surface Area Analysis

The specific surface area of GO and NHC-Pd@GO heterogeneous catalyst was measured by Brunauer–Emmet–Teller (BET) analysis which is based on the adsorption and desorption of nitrogen gas molecules on the solid surface. The nitrogen adsorption and desorption isotherms for (a) GO and (b) NHC-Pd@GO heterogeneous catalyst are shown in the Fig. 4. The amount of nitrogen adsorption on GO is high compared to that on the NHC-Pd@GO heterogeneous catalyst. The surface areas of bare GO was found to be 44.12 m^2g^{-1} which has got decreased to 6.23 m^2g^{-1} upon formation of the NHC-Pd@GO heterogeneous catalyst. The decrease in surface area discloses the successful functionalization of GO with the NHC-palladium(II) complex, which is evident from the BET data.

3.6 TEM Analysis

The TEM images of GO and NHC-Pd@GO catalyst are shown in Fig. 5a and b. The TEM image of the synthesized GO possesses thin transparent sheet like surface morphology with the presence of oxygen-containing functional groups attached on both sides of the sheet. Whereas the TEM image of newly synthesized NHC-Pd@GO heterogeneous catalyst displays a crumpled and layered like structure revealing the

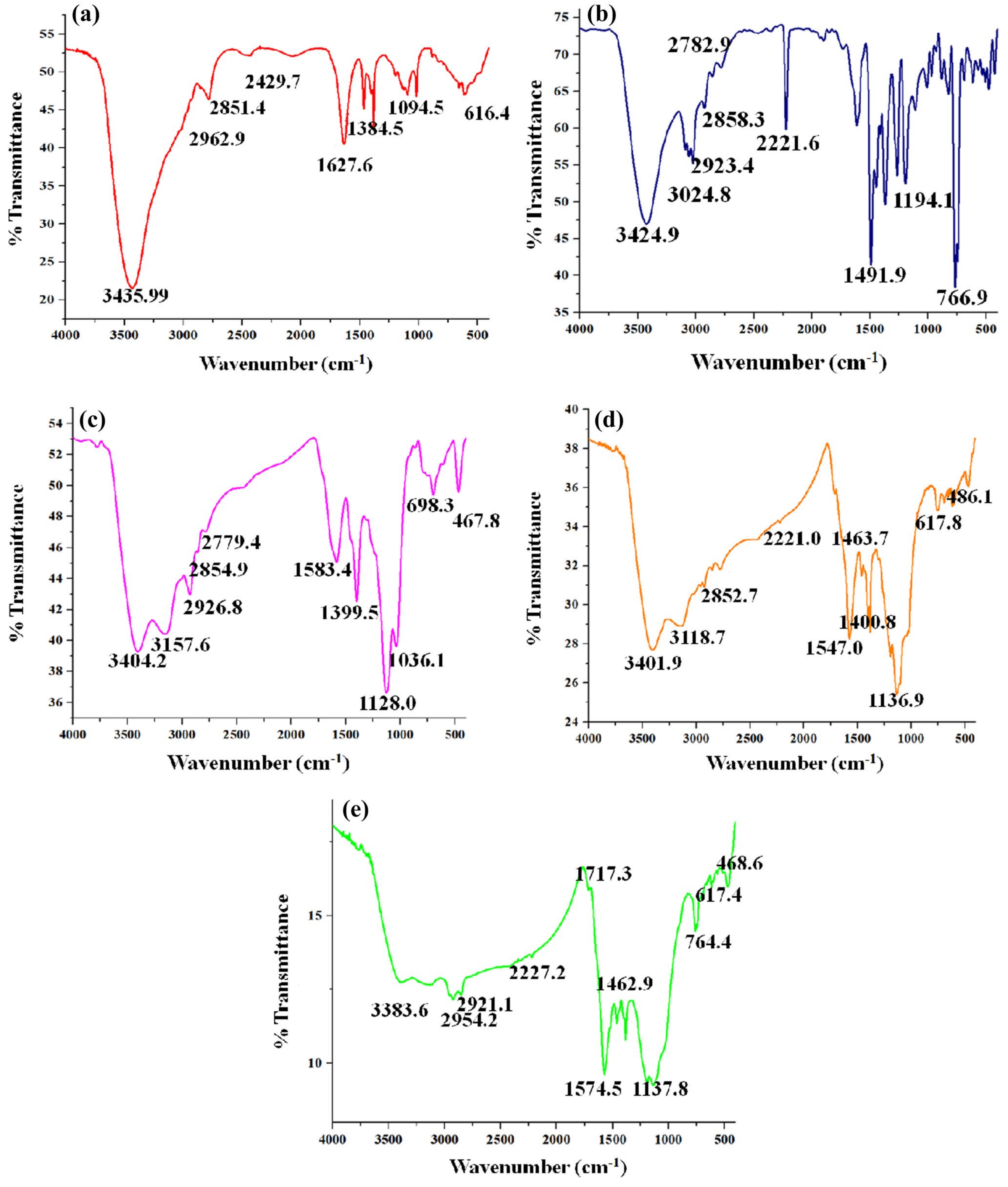

Fig. 1 FTIR spectra of **a** GO, **b** 4′-((1*H*-benzo[d]imidazol-1-yl)methyl)-[1,1′-biphenyl]-2-carbonitrile, **c** silane functionalized GO, **d** NHC@GO and **e** NHC-Pd@GO heterogeneous catalyst

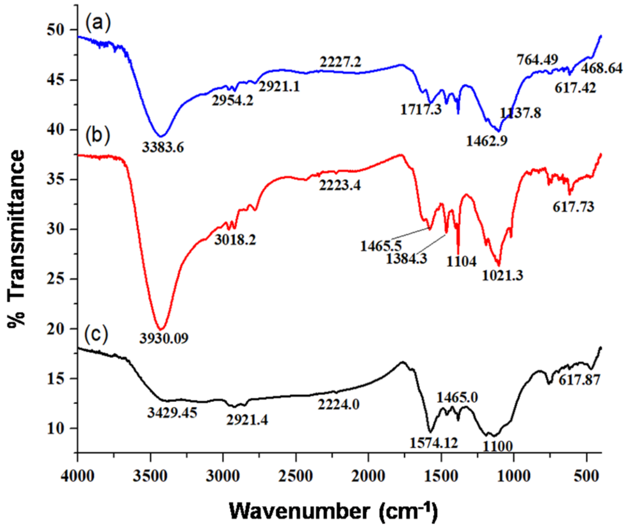

Fig. 2 FTIR spectra of NHC-Pd@GO heterogeneous catalyst: a freshly prepared, b recycled after Suzuki–Miyaura cross-coupling reaction and c recycled after nitroarene reduction

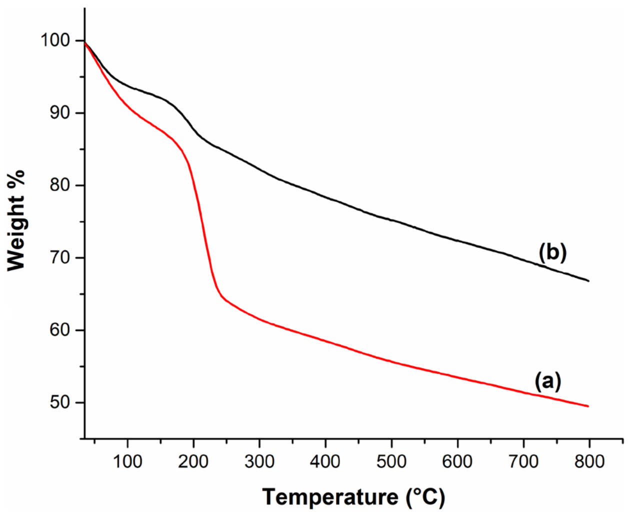

Fig. 3 TGA curves of a GO and b NHC-Pd@GO heterogeneous catalyst

successful synthesis of the NHC-Pd@GO heterogeneous catalyst.

3.7 FESEM Analysis

FESEM analysis was carried out to get more information about surface morphology of GO, NHC-Pd@GO heterogeneous catalyst, 12-times recycled NHC-Pd@GO heterogeneous catalyst in Suzuki–Miyaura reaction and ten-times recycled NHC-Pd@GO heterogeneous catalyst in reduction reaction. FESEM images are shown in Fig. 6. The FESEM images of the GO (Fig. 6a) and freshly prepared NHC-Pd@GO heterogeneous catalyst (Fig. 6b) demonstrated that both contain similar form, having two-dimensional nanosheets with wave-like structures. After 12-times and ten-times recycle in Suzuki–Miyaura cross-coupling and reduction of nitroarene, the surface morphology of the NHC-Pd@GO heterogeneous catalysts remained almost same as that of freshly prepared NHC-Pd@GO heterogeneous catalyst as depicted in Fig. 6c and d.

3.8 EDS Analysis

To confirm the elemental composition present in the newly synthesized NHC-Pd@GO heterogeneous catalyst, energy-dispersive X-ray spectroscopy (EDS) was employed. EDS spectra (Fig. 7) for NHC-Pd@GO heterogeneous catalyst shows different characteristic signals corresponding to C, N, O, Si, Cl, Pd atoms which defines the formation of NHC-Pd(II) complex on the surface of GO. Elemental mapping of the NHC-Pd@GO heterogeneous catalyst was carried out to understand the distribution of elements in the NHC-Pd@GO heterogeneous catalyst as shown in the Fig. 8. From elemental mapping it can be observed that all the elements are distributed evenly.

3.9 ICP-OES Analysis

Furthermore, the exact amount of palladium loading on newly synthesized NHC-Pd@GO heterogeneous catalyst was determined through ICP-OES analysis. The palladium loading of the NHC-Pd@GO heterogeneous catalyst was found to be 4.72% w/w by ICP-OES.

3.10 XRD Analysis

The crystalline nature of obtained GO and NHC-Pd@GO heterogeneous catalyst was analyzed through the powder XRD technique. The diffraction patterns of GO and NHC-Pd@GO are depicted in Fig. 9. The XRD pattern of GO (Fig. 9a) demonstrates the characteristic diffraction peak at $2\theta = 11.99°$ corresponding to (001) plane which is due to the introduction of oxygenic functional groups and trapped water molecules between the layers of GO. After immobilization of the NHC-palladium(II) complex, the peak (at $2\theta = 11.99°$) was disappeared and one more broad diffraction peak at $2\theta = 23.84°$ emerged, confirming that the major oxygen-containing groups of GO have been successfully functionalized (Fig. 9b).

3.11 Catalytic Activity of NHC-Pd@GO Heterogeneous Catalyst in Suzuki–Miyaura Cross-Coupling Reactions

The obtained NHC-Pd@GO heterogeneous catalyst was stable in air and moisture. After the characterization of

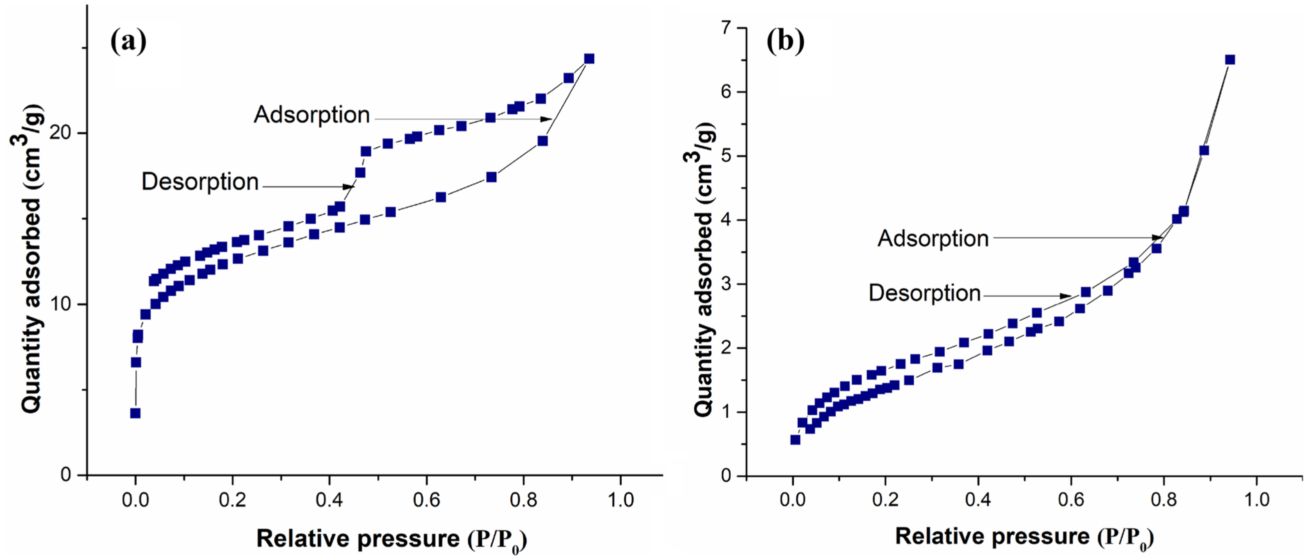

Fig. 4 Nitrogen adsorption–desorption curves for **a** GO and **b** NHC-Pd@GO heterogeneous catalyst

Fig. 5 TEM images of **a** GO, **b** NHC-Pd@GO heterogeneous catalyst

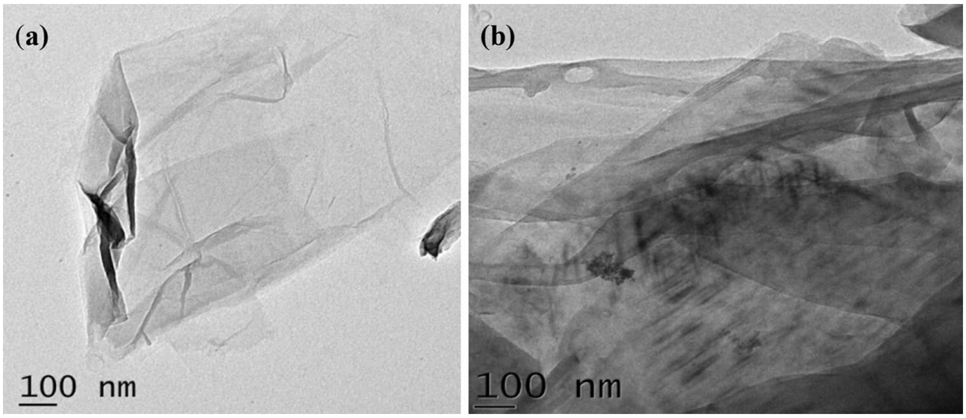

newly synthesized NHC-Pd@GO heterogeneous catalyst through spectroscopic and microscopic techniques, the catalytic activity was investigated initially for the Suzuki–Miyaura cross-coupling reaction. In the beginning, reaction conditions were optimized on a model Suzuki–Miyaura cross-coupling reaction between 4-bromobenzonitrile and phenylboronic acid as shown in Scheme 2. Much attention is given in solvent selection for any chemical transformation nowadays because of the environmental concern. Hence, during the optimization of reaction conditions, environmentally benign solvents like ethanol and water were given precedence. The reaction conditions were optimized through a series of model Suzuki–Miyaura cross-coupling reactions in the presence of NHC-Pd@GO heterogeneous catalyst as shown in Table 1. The preliminary results shown that using K_2CO_3 base, EtOH:H_2O (1:1) solvent, NHC-Pd@GO heterogeneous catalyst (10 mg) at room temperature for 1 h resulted in the highest yield (Table 1, entry 6). The catalytic activity of the NHC-Pd@GO heterogeneous catalyst with varying base, solvent, temperature, time, and catalyst ratio were also investigated for model reaction as shown in Tables 2, 3, 4, 5 and 6 respectively.

3.12 Effect of Base on Suzuki–Miyaura Cross-Coupling Reaction

The influence of base on the catalytic activity of NHC-Pd@GO heterogeneous catalyst was examined on model reaction using different bases: NaOH, KOH, $Na_3PO_4 \cdot 12H_2O$, Et_3N, KF, K_2CO_3, Na_2CO_3 and Cs_2CO_3 (Table 2). Among the bases employed, K_2CO_3 exhibited a good conversion rate (Table 2, entry 6) and remaining base NaOH, KOH, $Na_3PO_4 \cdot 12H_2O$, Et_3N, KF, Na_2CO_3 and Cs_2CO_3 resulted in lesser conversion (Table 2, entries 1–5 and entry 7–8).

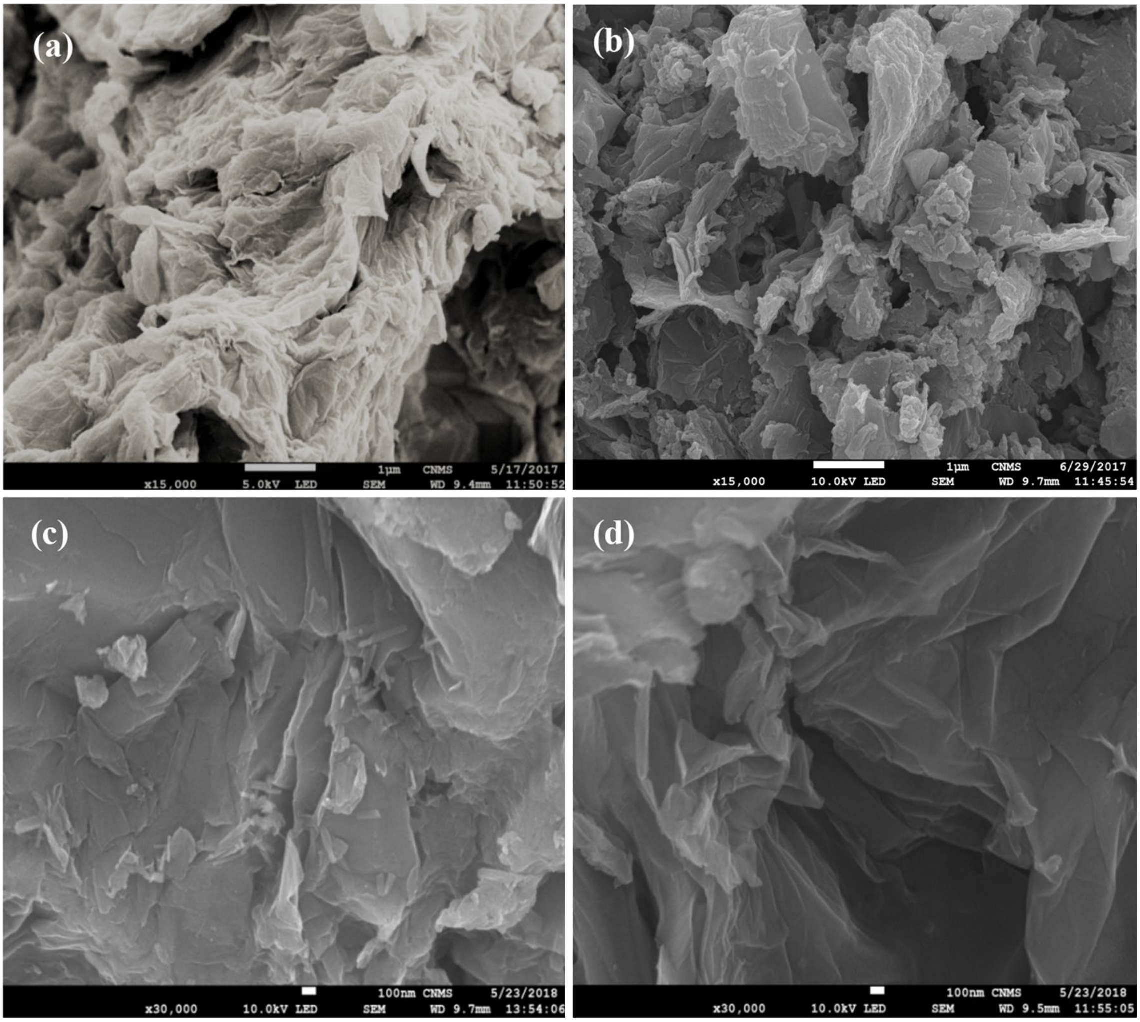

Fig. 6 FESEM images of **a** GO, **b** NHC-Pd@GO heterogeneous catalyst, **c** 12 times-recycled NHC-Pd@GO heterogeneous catalyst in Suzuki–Miyaura cross-coupling reaction and **d** ten times recycled NHC-Pd@GO heterogeneous catalyst in reduction reaction

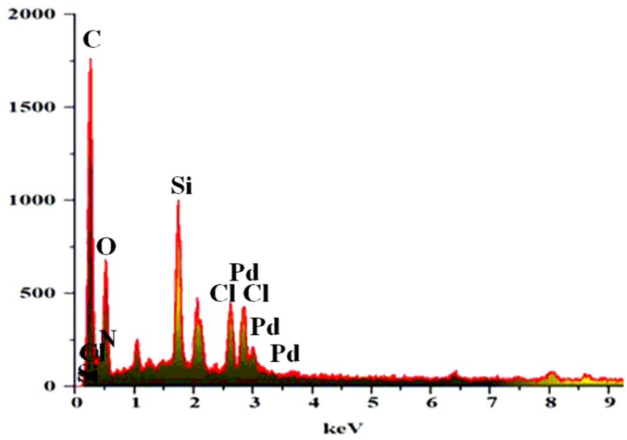

Fig. 7 EDS-spectrum of NHC-Pd@GO heterogeneous catalyst

3.13 Effect of Solvent on Suzuki–Miyaura Cross-Coupling Reaction

The catalytic potential of NHC-Pd@GO heterogeneous catalyst in different solvents were investigated with different solvents such as acetone, DCM, toluene, THF, H_2O, EtOH, EtOH:H_2O (1:1) and isopropyl alcohol. From the results obtained as shown in Table 3, it is clear that reaction did not proceed in acetone and THF (Table 3, entries 1 and 4). When DMF, toluene, ethanol and isopropyl alcohol were used cross-coupled product yield was medium (Table 3, entries 2, 3, 6 and 8). Furthermore, the model reaction in EtOH-H_2O (1:1) mixture gave the highest yield (Table 3, entry 7).

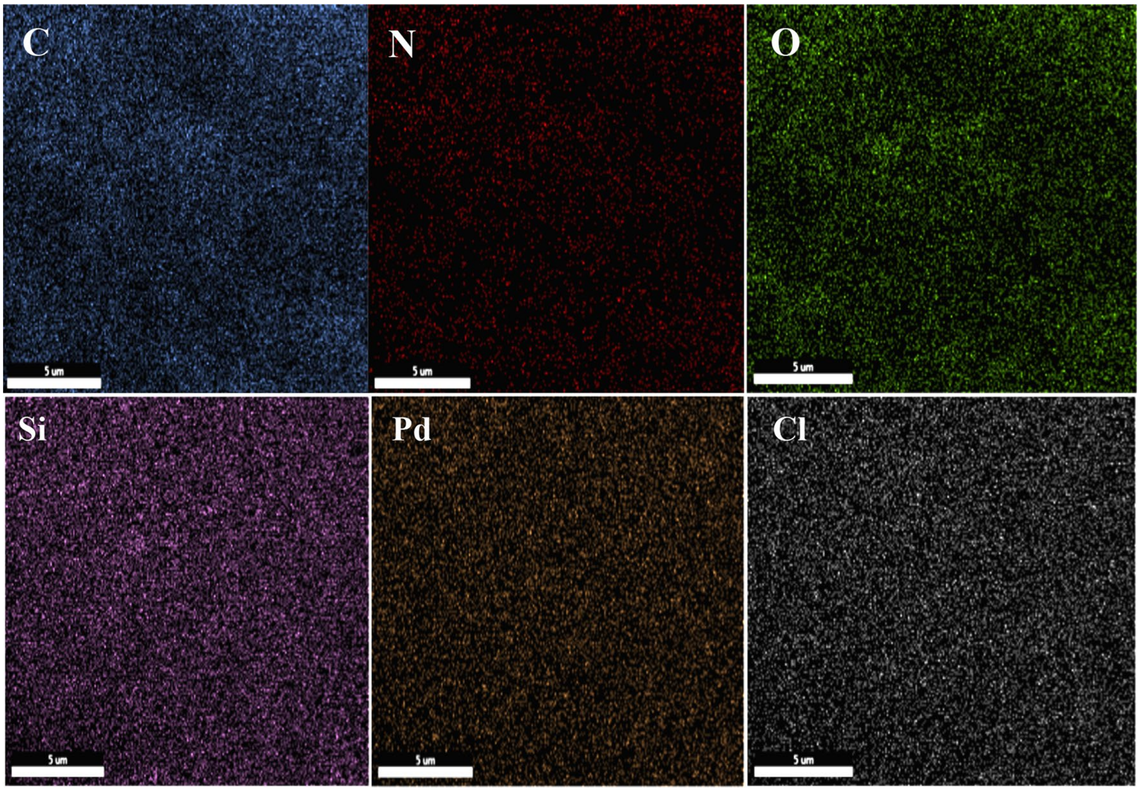

Fig. 8 Elemental mapping of NHC-Pd@GO heterogeneous catalyst

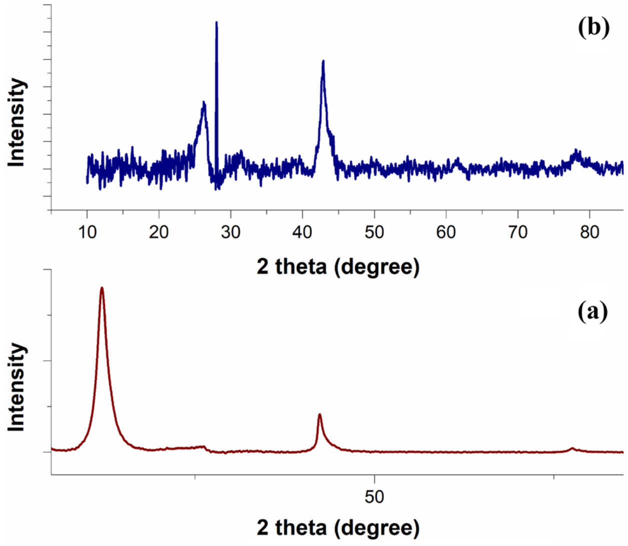

Fig. 9 XRD pattern of **a** GO and **b** NHC-Pd@GO heterogeneous catalyst

3.14 Effect of Temperature on Suzuki–Miyaura Cross-Coupling Reaction

To find out the temperature effect in the catalytic activity of newly prepared NHC-Pd@GO heterogeneous catalyst, model reaction was carried out at different temperatures as depicted in Table 4. Results demonstrate that the NHC-Pd@GO heterogeneous catalyst is highly active at room temperature itself (Table 4, entry 1) and hence it is preferred over higher temperatures even though there is no difference in the yield (Table 4, entries 2–4).

3.15 Effect of Time on Suzuki–Miyaura Cross-Coupling Reaction

To investigate the time effect, the model Suzuki–Miyaura cross-coupling reaction was conducted at different time intervals in the presence of NHC-Pd@GO heterogeneous catalyst (Table 5). It is understood from the results obtained that the yield of reaction increased with increase in time upto 1 h (Table 5, entries 1–4) and further yield improvement was not observed (Table 5, entries 5–7). Hence, 1 h is the optimum time required for the maximum yield (Table 5, entry 4).

3.16 Effect of Catalyst Ratio on Suzuki–Miyaura Cross-Coupling Reaction

The optimal amount of the NHC-Pd@GO heterogeneous catalyst required in the Suzuki–Miyaura cross-coupling reaction has to be determined for the effective utilization of it in any

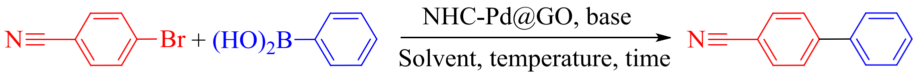

Scheme 2 Suzuki–Miyaura cross-coupling reaction of 4-bromobenzonitrile with phenylboronic acid

Table 1 Optimization of reaction conditions for model Suzuki–Miyaura cross-coupling reaction in the presence of NHC-Pd@GO heterogeneous catalyst

Entry	Base	Solvent	Temp. (°C)	Time (h)	Yield (%)[a]
1	K_2CO_3	MeOH	R.T	7	80
2	K_2CO_3	H_2O	R.T	12	40
3	K_2CO_3	EtOH	R.T	5	70
4	K_2CO_3	DMF	R.T	12	50
5	K_2CO_3	CH_3CN	R.T	12	Trace
6	**K_2CO_3**	**EtOH:H_2O**	**R.T**	**1**	**98**
7	K_2CO_3	EtOH:H_2O	R.T	2	98
8	K_2CO_3	EtOH:H_2O	R.T	0.5	90
9	Na_2CO_3	EtOH:H_2O	R.T	1	90
10	Na_2CO_3	EtOH:H_2O	R.T	2	95

Reaction conditions: 4-bromobenzonitrile (0.27 mmol), phenylboronic acid (0.30 mmol), NHC-Pd@GO catalyst (0.02 mol % Pd with respect to aryl halide), base (0.60 mmol) and solvent (5 mL) in air

The best reaction condition with the highest yield is given in bold

[a] Isolated yield

organic transformation. The study of effect of catalyst loading in the model Suzuki–Miyaura cross-coupling reaction is shown in Table 6. The quantity of NHC-Pd@GO heterogeneous catalyst was varied and studied for catalyst ratios with 0.01, 0.02, 0.03, 0.04, 0.05 mol% of Pd in the model reaction (Table 6, entries 1–5). The yield of the biaryl product increased with the catalyst loading (Table 6, entries 1 and 2). A high yield of 98% was obtained when 0.02 mol % Pd was used (Table 6, entry 2) and further increase in the catalyst ratio did not increase the yield (Table 6, entries 3–5).

3.17 Suzuki–Miyaura Cross-Coupling Reactions of Substituted Aryl Halides with Phenylboronic Acid

The Suzuki–Miyaura cross-coupling reaction is one of the most imperative methods for C–C bond formation in organic reaction. The Suzuki–Miyaura cross-coupling reaction is used in the synthesis of broad range of C–C coupled products and therefore it belongs to a vital set of palladium catalyzed cross-coupling reactions. Hence, catalytic potential of the NHC-Pd@GO heterogeneous catalyst was tested in Suzuki–Miyaura cross-coupling reactions of different aryl halides with phenylboronic acid using the optimized conditions and the results are tabulated in Table 7. The investigational procedure is simple and convenient, and has the capability to tolerate a wide range of functional groups. All the cross-coupled products were isolated and purified by column chromatography. The obtained results disclose that electronically diverse substituted aryl bromides and aryl iodides are converted into the corresponding products in good to excellent yields (Table 7, entries 1–15). However, aryl bromides (Table 7, entries 1–10) reacted slowly than the iodide derivatives (Table 7, entries 11–15). Conversely, reaction of aryl chloride with phenylboronic acid gave cross-coupling products in low yield (Table 7, entry 16). In contrast, selectivity

Table 2 Suzuki–Miyaura cross-coupling reaction of model reaction in the presence of NHC-Pd@GO heterogeneous catalyst with different bases

Entry	Base	Solvent	Temp. (°C)	Time (h)	Yield (%)[a]
1	NaOH	EtOH:H_2O	R.T	4	20
2	KOH	EtOH:H_2O	R.T	8	95
3	$Na_3PO_4 \cdot 12H_2O$	EtOH:H_2O	R.T	4	95
4	Et_3N	EtOH:H_2O	R.T	3	60
5	KF	EtOH:H_2O	R.T	4	50
6	**K_2CO_3**	**EtOH:H_2O**	**R.T**	**1**	**98**
7	Cs_2CO_3	EtOH:H_2O	R.T	1	90
8	Na_2CO_3	EtOH:H_2O	R.T	1	90

Reaction conditions: 4-bromobenzonitrile (0.27 mmol), phenylboronic acid (0.30 mmol), NHC-Pd@GO heterogeneous catalyst (0.02 mol % Pd with respect to aryl halide), base (0.60 mmol) and solvent (5 mL) in air

The best reaction condition with the highest yield is given in bold

[a] Isolated yield

Table 3 Suzuki–Miyaura cross-coupling reaction of model reaction in the presence of NHC-Pd@GO heterogeneous catalyst with various solvents

Entry	Base	Solvent	Temp. (^oC)	Time (h)	Yield (%)[a]
1	K_2CO_3	Acetone	R.T	12	Trace
2	K_2CO_3	DMF	R.T	12	30
3	K_2CO_3	Toluene	R.T	3	30
4	K_2CO_3	THF	R.T	7	Trace
5	K_2CO_3	H_2O	R.T	12	40
6	K_2CO_3	EtOH	R.T	5	70
7	**K_2CO_3**	**EtOH:H_2O**	**R.T**	**1**	**98**
8	K_2CO_3	IPA	R.T	7	70

Reaction conditions: 4-bromobenzonitrile (0.27 mmol), phenylboronic acid (0.30 mmol), NHC-Pd@GO heterogeneous catalyst (0.02 mol % Pd with respect to aryl halide), base (0.60 mmol) and solvent (5 mL) in air

The best reaction condition with the highest yield is given in bold

[a] Isolated yield

Table 4 Suzuki–Miyaura cross-coupling reaction of model reaction in the presence of NHC-Pd@GO heterogeneous catalyst at various temperatures

Entry	Base	Solvent	Temp. (^oC)	Time (h)	Yield (%)[a]
1	**K_2CO_3**	**EtOH:H_2O**	**R.T**	**1**	**98**
2	K_2CO_3	EtOH:H_2O	40	1	98
3	K_2CO_3	EtOH:H_2O	50	1	98
4	K_2CO_3	EtOH:H_2O	60	1	97

Reaction conditions: 4-bromobenzonitrile (0.27 mmol), phenylboronic acid (0.30 mmol), NHC-Pd@GO heterogeneous catalyst (0.02 mol % with respect to aryl halide), base (0.60 mmol) and solvent (5 mL) in air

The best reaction condition with the highest yield is given in bold

[a] Isolated yield

of the NHC-Pd@GO heterogeneous catalyst was established through the existence of a negligible amount of the homocoupled product obtained. For more explanation on selectivity, Suzuki–Miyaura cross-coupling reactions were carried out without aryl halides under optimized conditions. The biphenyl homocoupled product obtained was in trace amount, which concluded that the NHC-Pd@GO heterogeneous catalyst is highly selective. Moreover, a plausible mechanism for our newly synthesized NHC-Pd@GO heterogeneous catalyst is demonstrated in Scheme 3 which gives the C–C cross-coupling products via possible mechanistic intermediates (**I–III**).

Table 5 Suzuki–Miyaura cross-coupling reaction of model reaction in the presence of NHC-Pd@GO heterogeneous catalyst at various time intervals

Entry	Base	Solvent	Temp. (^oC)	Time (h)	Yield (%)[b]
01	K_2CO_3	EtOH:H_2O	R.T	0.25	80
02	K_2CO_3	EtOH:H_2O	R.T	0.50	90
03	K_2CO_3	EtOH:H_2O	R.T	0.75	95
04	**K_2CO_3**	**EtOH:H_2O**	**R.T**	**1.00**	**98**
05	K_2CO_3	EtOH:H_2O	R.T	1.50	98
06	K_2CO_3	EtOH:H_2O	R.T	1.75	98
07	K_2CO_3	EtOH:H_2O	R.T	2.00	98

Reaction conditions: 4-bromobenzonitrile (0.27 mmol), phenylboronic acid (0.30 mmol), NHC-Pd@GO heterogeneous catalyst (0.02 mol % with respect to aryl halide), base (0.60 mmol) and solvent (5 mL) in air

The best reaction condition with the highest yield is given in bold

[a] Isolated yield

Table 6 Suzuki–Miyaura cross-coupling reaction of model reaction in the presence of NHC-Pd@GO heterogeneous catalyst with different catalyst ratios

Entry	Base	Pd (mol %)	Temp. (^oC)	Time (h)	Yield (%)[a]
1	K_2CO_3	0.01	R.T	1	85
2	**K_2CO_3**	**0.02**	**R.T**	**1**	**98**
3	K_2CO_3	0.03	R.T	1	98
4	K_2CO_3	0.04	R.T	1	96
5	K_2CO_3	0.05	R.T	1	93

Reaction conditions: 4-bromobenzonitrile (0.27 mmol), phenylboronic acid (0.30 mmol), base (0.60 mmol) and solvent (5 mL) in air

The best reaction condition with the highest yield is given in bold

[a] Isolated yield

3.18 Catalyst Recyclability Study in Suzuki–Miyaura Cross-Coupling Reactions

The recyclability study of NHC-Pd@GO was carried out on the model Suzuki–Miyaura cross-coupling reaction. The prepared catalyst shown good activity upto 11 recycles

Table 7 Suzuki–Miyaura cross-coupling reactions of different aryl halides with phenylboronic acid catalyzed by NHC-Pd@GO heterogeneous catalyst

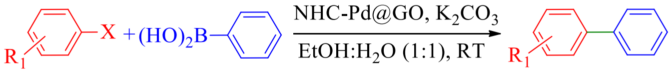

Entry	Aryl halide	Product	Time (h)	Yield (%)^b
01	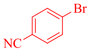	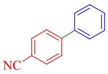	1	98
02	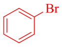	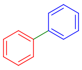	1	96
03	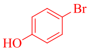	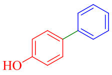	2	90
04	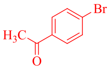	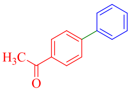	2	85
05	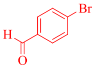	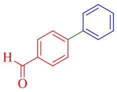	1	88
06	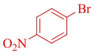	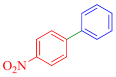	1	98
7	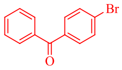	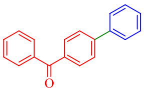	8	75
8	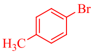	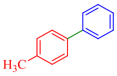	2	92
9	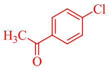	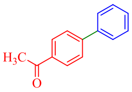	5	45
10	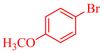	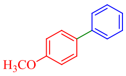	2	91
11	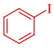	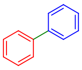	1	98
12	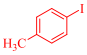	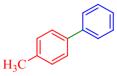	1	96
13	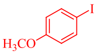	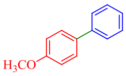	1	94
14	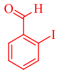	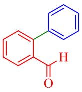	1	94
15	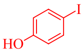	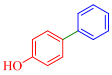	1	95
16	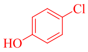	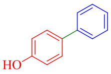	12	50

Reaction conditions: aryl halide (0.27 mmol), phenylboronic acid (0.30 mmol), NHC-Pd@GO heterogeneous catalyst (0.02 mol% Pd), base (0.60 mmol) and EtOH-H_2O (5 mL) in air

[a] Isolated yield after separation by column chromatography; average of two runs

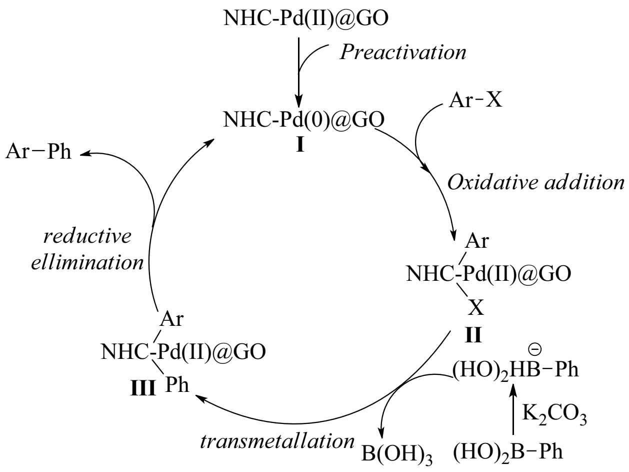

Scheme 3 Proposed mechanism of Suzuki–Miyaura cross-coupling reaction

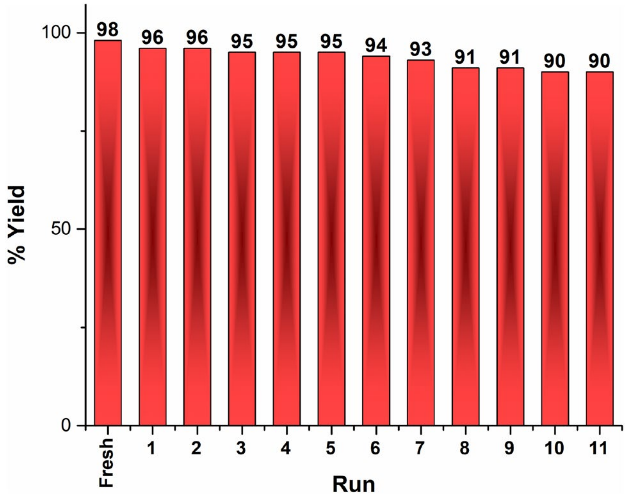

Fig. 10 Recycling efficiency of NHC-Pd@GO heterogeneous catalyst in Suzuki–Miyaura cross-coupling reaction

as shown in Fig. 10. Also, it is observed that there is a slow and steady decrease in the activity from sixth recycle onwards which may be due to the blocking of active sites on the catalyst by reactant left over even though the washings of the recovered catalyst were performed.

3.19 Comparison of Catalysts

In order to understand the advantages and disadvantages and to scrutinize how important is NHC-Pd@GO heterogeneous catalyst among the reported catalysts in Suzuki–Miyaura cross-coupling reaction, we have compared the yields obtained from our protocol with other related protocols which is given in Table 8. From this table it can be concluded that NHC-Pd@GO heterogeneous catalyst showed good to excellent activity when compared with other catalytic systems.

3.20 Activity of NHC-Palladium(II) Grafted Graphene Oxide Catalyst in Reduction of Nitroarenes

Subsequent to the catalytic activity study of NHC-Pd@GO in Suzuki–Miyaura cross-coupling, the prepared catalyst was studied for its activity in reduction of nitroarenes. The reduction of nitrobenzene to aniline was chosen as the model reaction to optimize the reaction conditions (Scheme 4). The reaction conditions were optimized through a series of reaction by varying conditions like solvent, reducing agent ratio, and temperature and so on as shown in Table 9. The solvent choice was predetermined to be aqueous and green and hence aqueous ethanol and methanol were only studied for solvent system. The reaction yield was less when only water was used as solvent which may be due to the low solubility of the starting material in water. The optimal ratio of sodium borohydride was found to be two equivalents. An increase in the ratio of sodium borohydride resulted in no change where as decrease in the ratio resulted in lower yields of the product. Also, an increase or decrease in catalyst ratio from 0.003 mol% of Pd resulted in lower yields. The optimized condition obtained for reduction was by using 2 equivalent reducing agent ($NaBH_4$) and 1:1 ratio of MeOH:H_2O solvent (5 mL) in presence of 0.003 Pd mol % catalyst at room temperature in ten minutes.

3.21 Reduction of Various Nitroarenes

With the optimized conditions available, we then proceeded to study the reduction of different nitroarenes as shown in the Table 10. The range of substrates studied contained different electron withdrawing as well as electron donating groups. The NHC-Pd@GO could catalyze the reduction of nitroarenes in good to excellent conversion rates and yield in less time duration under optimized conditions. The use of eco-friendly solvent at room temperature in less time is a few advantages of the protocol presented here. Furthermore, a plausible mechanism for the reduction of nitroarene using $NaBH_4$ catalysed by NHC-Pd@GO heterogeneous catalyst through probable mechanistic intermediates (**I**–**V**) is given in Scheme 5.

3.22 Catalyst Recyclability in Nitroarene Reduction

Recyclability study of NHC-Pd@GO heterogeneous catalyst was also carried out for the model reaction in nitroarene reduction under optimized conditions. The

Table 8 Comparison of results in Suzuki–Miyaura cross-coupling reaction between 4-bromotoluene and phenylboronic acid using NHC-Pd@GO heterogeneous catalyst with other reported catalysts

Entry	Catalyst	Solvent	Temp. (°C)	Time (h)	Yield (%)	Refs.
1	GO-2*N*-Pd(II)	EtOH	80	4	77	[35]
2	GO-CPTMS-Pd	$EtOH:H_2O$ (2:1)	80	3	95	[43]
3	NHC-Pd/GO-IL	$EtOH:H_2O$ (1:1)	60	2.5	85	[44]
4	GO-NHC-Pd^{2+}	$EtOH:H_2O$ (1:1)	80	20	94	[45]
5	Catalyst	$EtOH:H_2O$ (1:1)	R.T	1	99	[46]
6	GO-NHC-Pd^{2+}	$EtOH:H_2O$ (2:1)	60	4	70	[47]
7	**NHC-Pd@GO**	**$EtOH:H_2O$ (1:1)**	**R.T**	**1**	**92**	Present work

The best reaction condition with the highest yield is given in bold

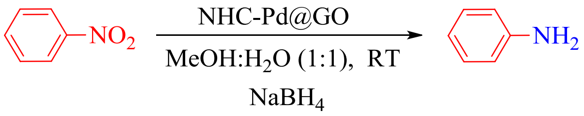

Scheme 4 Catalytic activity of NHC-Pd@GO heterogeneous catalyst in reduction of nitrobenzene

NHC-Pd@GO heterogeneous catalyst was recovered by the centrifugation of reaction medium after reaction completion. Separated catalyst was then washed with methanol (2 × 10 mL) followed by water (10 mL) and dried at 40 °C in hot oven. Further, the recovered catalyst was reused for reduction of nitroarenes and it was observed that there was no change in catalytic activity up to ten recycles as shown in Fig. 11.

3.23 Comparison of Catalysts

A comparison data of the catalytic activity of NHC-Pd@GO heterogeneous catalyst with other reported catalyst in nitroarene reduction was also carried out which is shown in Table 11. The comparison data reveals that NHC-Pd@GO heterogeneous catalyst performed with comparable product yields in the reduction reaction with the additional merits of usage of environmentally benign solvent, mild reaction conditions and less time period for reaction completion.

3.24 Heterogeneity Study

In order to confirm the heterogeneity of NHC-Pd@GO, leaching study was carried out for the model Suzuki–Miyaura cross-coupling reaction. Here, the reaction mass containing NHC-Pd@GO heterogeneous catalyst and the base was stirred for one hour and filtered before the addition of aryl halide and phenylboronic acid. After the removal of NHC-Pd@GO heterogeneous catalyst, aryl halide and phenylboronic acid were added to the filtrate and allowed to stir for another one hour and the reaction was monitored by TLC and found that there is no product formation and the reactants remained unreacted. This study confirms that there is no palladium in the soluble form which is leaching out from the catalyst to reaction mass. Thus, it proves that NHC-Pd@GO heterogeneous catalyst is heterogeneous in nature.

Table 9 Optimization of reaction conditions for the reduction of nitrobenzene in presence of NHC-Pd@GO heterogeneous catalyst

Entry	Solvent	$NaBH_4$ ratio	Pd (mol %)	Time (h)	Yield (%)[a]
01	H_2O	3	0.006	0.16	60
02	$MeOH:H_2O$	3	0.006	0.16	95
03	$MeOH:H_2O$	3	0.003	0.16	95
04	$MeOH:H_2O$	3	0.009	0.16	93
05	$MeOH:H_2O$	3	0.002	0.16	75
06	$MeOH:H_2O$	1	0.003	0.16	70
07	**$MeOH:H_2O$**	**2**	**0.003**	**0.16**	**95**
08	MeOH	2	0.003	0.16	Trace
09	EtOH	2	0.003	0.16	Trace
10	EtOH:H2O	2	0.003	0.16	60

Reaction conditions: nitrobenzene (0.81 mmol) and solvent 10 mL

The best reaction condition with the highest yield is given in bold

[a] Isolated yield

Table 10 Nitroarenes reduction catalyzed by NHC-Pd@GO heterogeneous catalyst

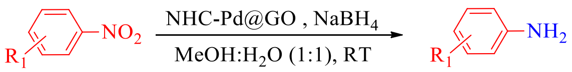

Entry	Nitroarenes	Product	Temp (°C)	Time (h)	Yield (%)[b]
01	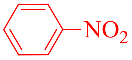	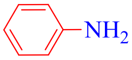	RT	0.16	95
02	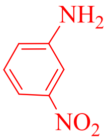	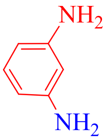	RT	0.16	90
03	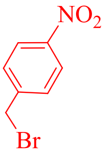	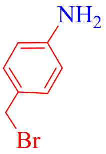	RT	0.16	Trace
04	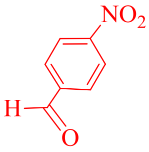	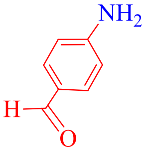	RT	0.16	90
05	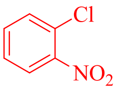	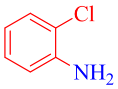	RT	0.16	65
06	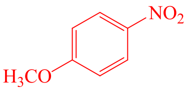	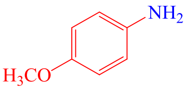	RT	0.16	95
07	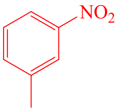	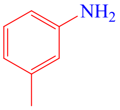	RT	0.16	80

Reaction conditions: nitrobenzene (0.81 mmol), sodium borohydride (1.6 mmol) and catalyst (0.003 Pd mol% with respect to nitroarenes) and solvent 10 mL

[a] Isolated yield after separation by column chromatography; average of two runs

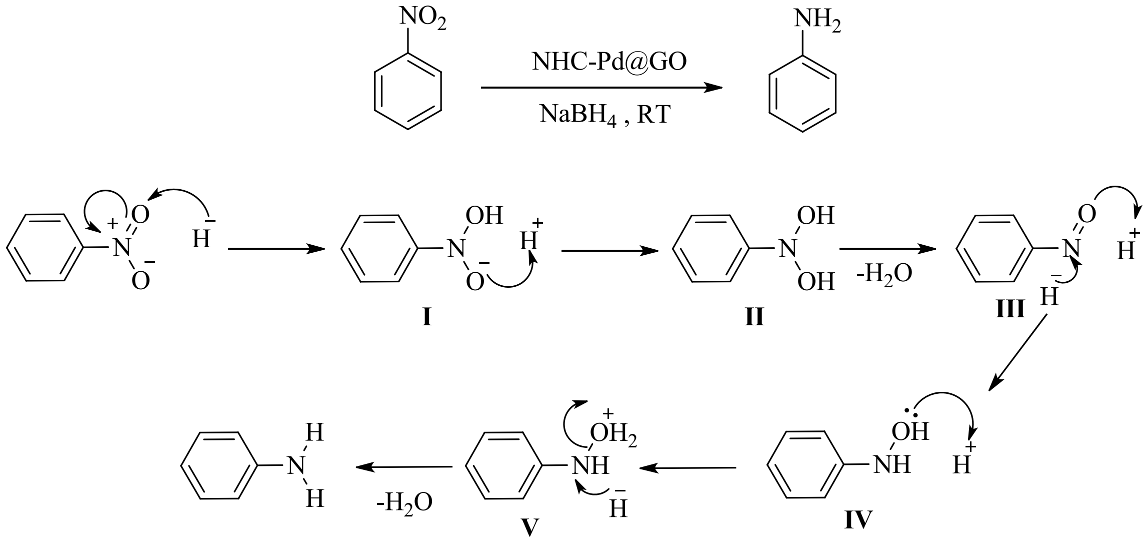

Scheme 5 Proposed mechanism for reduction of nitroarene using $NaBH_4$ catalysed by NHC-Pd@GO nanomagnetic catalyst

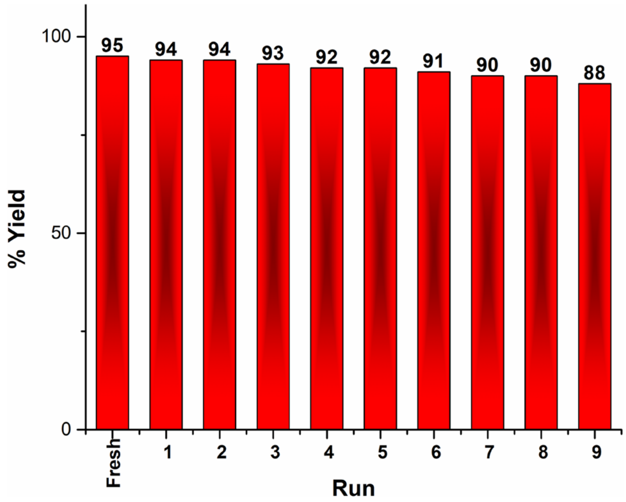

Fig. 11 Recycling efficiency of NHC-Pd@GO heterogeneous catalyst in nitroarene reduction

4 Conclusions

In summary, NHC-Pd@GO heterogeneous catalyst was successfully prepared and characterized by FTIR spectroscopy, TGA, BET, TEM, FESEM, EDS, ICP-OES and XRD analysis. The new NHC-Pd@GO heterogeneous catalyst showed good catalytic activity in both Suzuki–Miyaura cross-coupling reaction and reduction of nitroarenes. The main advantages of this catalyst are its simple design, eco-friendliness and recyclability. The recovered catalyst can be reused up to eleven recycles without significant loss of catalytic activity in Suzuki–Miyaura cross-coupling reactions and up to nine recycles in case of nitroarenes reduction. The novel NHC-based palladium complexes can be prepared and immobilized on graphene oxide following this protocol which can be used in various organic transformations like Mizoroki–Heck reaction, Sonogashira-Hagihara coupling reaction, oxidation reactions apart from Suzuki–Miyaura cross coupling and nitroarenes reduction.

Table 11 Comparison of results in nitrobenzene reduction using NHC-Pd@GO heterogeneous catalyst with other reported catalysts

Entry	Catalyst	Solvent	Temp. (°C)	Time (h)	Yield (%)	Refs.
1	Pd/C (5%)	THF:H_2O	60	3	85	[48]
2	Catalyst 1	MeOH	50	12	95	[49]
3	Pd-gCN	EtOH	70	4	99	[50]
4	PdNPs	H_2O:MeOH (2:1)	R. T	0.16	99	[51]
5	rGO-$Fe_{48}Pd_{52}$	H_2O:MeOH (3:7)	R. T	0.16	99	[52]
6	rGO@Ag/Pd	H_2O:MeOH (3:7)	R. T	0.08	99	[53]
7	**NHC-Pd@GO**	**H_2O:MeOH (1:1)**	**R. T**	**0.16**	**95**	Present work

The best reaction condition with the highest yield is given in bold

Acknowledgements The authors thank DST-SERB, India (YSS/2015/000010), DST-Nanomission, India (SR/NM/NS-20/2014), and Jain University, India for financial support.

Compliance with Ethical Standards

Conflict of interest All authors declares that they have no conflicts to declare.

References

1. Miyaura N, Suzuki A (1995) Chem Rev 95:2457–2483
2. Suzuki A (2011) Angew Chem Int Ed Engl 50:6722–6737
3. Chinchilla R, Najera C (2011) Chem Soc Rev 40:5084–5121
4. Yin L, Liebscher J (2007) Chem Rev 107:133–173
5. Magano J, Dunetz JR (2011) Chem Rev 111:2177–2250
6. Phan NTS, Van Der Sluys M, Jones CW (2006) Adv Synth Catal 348:609–679
7. Corbet JP, Mignani G (2006) Chem Rev 106:2651–2710
8. Hassan J, Sevignon M, Gozzi C, Schulz E, Lemaire M (2002) Chem Rev 102:1359–1470
9. Belardi JK, Micalizio GC (2008) Angew Chem Int Ed Engl 47:4005–4008
10. Jia Y, Bois-Choussy M, Zhu J (2008) Angew Chem Int Ed Engl 47:4167–4172
11. Stanforth SP (1998) Tetrahedron 54:263–303
12. Herrmann WA (2002) Angew Chem Int Ed Engl 41:1290–1309
13. Botella L, Najera C (2002) Angew Chem Int Ed Engl 41:179–181
14. Grasa GA, Hillier AC, Nolan SP (2001) Org Lett 3:1077–1080
15. Old DW, Wolfe JP, Buchwald SL (1998) J Am Chem Soc 120:9722–9723
16. Patil SA, Weng C-M, Huang P-C, Hong F-E (2009) Tetrahedron 65:2889–2897
17. Dewan A, Bora U, Borah G (2014) Tetrahedron Lett 55:1689–1692
18. Downing RS, Kunkeler PJ, van Bekkum H (1997) Catal Today 37:121–136
19. Junge K, Schroder K, Beller M (2011) Chem Commun 47:4849–4859
20. Linares C, Mediavilla M, Pardey AJ, Baricelli P, Pardey CL, Moya SA (1998) Catal Lett 50:183–185
21. Orlandi M, Tosi F, Bonsignore M, Benaglia M (2015) Org Lett 17:3941–3943
22. Yu C, Liu B, Hu L (2001) J Org Chem 66:919–924
23. Peris E (2018) Chem Rev 118:9988–10031
24. Marichev KO, Patil SA, Bugarin A (2018) Tetrahedron 74:2523–2546
25. Mpungose PP, Vundla ZP, Maguire GEM, Friedrich HB (2018) Molecules 23:1676–1700
26. Patil SA, Patil SA, Patil R (2016) J Nano Res 42:112–135
27. Zhong R, Lindhorst AC, Groche FJ, Kuhn FE (2017) Chem Rev 117:1970–2058
28. Wang W, Cui L, Sun P, Shi L, Yue C, Li F (2018) Chem Rev 118:9843–9929
29. Yang J, Wu Y, Wu X, Liu W, Wang Y, Wang J (2019) Green Chem 21:5267–5273
30. Dreyer DR, Park S, Bielawski CW, Ruoff RS (2010) Chem Soc Rev 39:228–240
31. Tan R, Li C, Luo J, Kong Y, Zheng W, Yin D (2013) J Catal 298:138–147
32. Szabó T, Berkesi O, Forgó P, Josepovits K, Sanakis Y, Petridis D, Dékány I (2006) Chem Mater 18:2740–2749
33. Guo S, Dong S, Wang E (2010) ACS Nano 4:547–555
34. Guo S, Sun S (2012) J Am Chem Soc 134:2492–2495
35. Bai C, Zhao Q, Li Y, Zhang G, Zhang F, Fan X (2014) Catal Lett 144:1617–1623
36. Khatri PK, Choudhary S, Singh R, Jain SL, Khatri OP (2014) Dalton Trans 43:8054–8061
37. Mungse HP, Verma S, Kumar N, Sain B, Khatri OP (2012) J Mater Chem 22:5427–5433
38. Vishal K, Fahlman BD, Sasidhar BS, Patil SA, Patil SA (2017) Catal Lett 147:900–918
39. Kandathil V, Fahlman BD, Sasidhar BS, Patil SA, Patil SA (2017) New J Chem 41:9531–9545
40. Manjunatha K, Koley TS, Kandathil V, Dateer RB, Balakrishna G, Sasidhar BS, Patil SA, Patil SA (2018) Appl Organomet Chem 32:e4266
41. Kandathil V, Koley TS, Manjunatha K, Dateer RB, Keri RS, Sasidhar BS, Patil SA, Patil SA (2018) Inorg Chim Acta 478:195–210
42. Kempasiddhaiah M, Kandathil V, Dateer RB, Sasidhar BS, Patil SA, Patil SA (2019) Appl Organomet Chem 33:e4846
43. Bahrami K, Targhan H (2019) Appl Organomet Chem 33:e4842
44. Movahed SK, Esmatpoursalmani R, Bazgir A (2014) RSC Adv 4:14586–14591
45. Shang N, Gao S, Feng C, Zhang H, Wang C, Wang Z (2013) RSC Adv 3:21863–21868
46. Qian Y, So J, Jung S-Y, Hwang S, Jin M-J, Shim S (2019) Synthesis 51:2287–2292
47. Shang N, Feng C, Zhang H, Gao S, Tang R, Wang C, Wang Z (2013) Catal Commun 40:111–115
48. Baron M, Métay E, Lemaire M, Popowycz F (2013) Green Chem 15:1006–1015
49. Yang S-T, Shen P, Liao B-S, Liu Y-H, Peng S-M, Liu S-T (2017) Organometallics 36:3110–3116
50. Nandi D, Siwal S, Choudhary M, Mallick K (2016) Appl Catal A 523:31–38
51. Patil NM, Bhosale MA, Bhanage BM (2015) RSC Adv 5:86529–86535
52. Metin Ö, Mendoza-Garcia A, Dalmızrak D, Gültekin MS, Sun S (2016) Catal Sci Technol 6:6137–6143
53. Metin O, Can H, Sendil K, Gultekin MS (2017) J Colloid Interface Sci 498:378–386